



The Role of Distal Dendritic Gap Junctions in Synchronization of Mitral Cell Axonal Output

M. MIGLIORE*

Department of Neurobiology, Yale University School of Medicine, New Haven, CT, USA; Institute of Biophysics, National Research Council, Palermo, Italy

michele.migliore@yale.edu

M.L. HINES AND GORDON M. SHEPHERD

Department of Neurobiology, Yale University School of Medicine, New Haven, CT, USA

Received June 8, 2004; Revised September 15, 2004; Accepted October 8, 2004

Action Editor: Roger Traub

Abstract. One of the first and most important stages of odor processing occurs in the glomerular units of the olfactory bulb and most likely involves mitral cell synchronization. Using a detailed model constrained by a number of experimental findings, we show how the intercellular coupling mediated by intraglomerular gap junctions (GJs) in the tuft dendrites could play a major role in synchronization of mitral cell action potential output in spite of their distal dendritic location. The model suggests that the high input resistance and active properties of the fine tuft dendrites are instrumental in generating local spike synchronization and an efficient forward and backpropagation of action potentials between the tuft and the soma. The model also gives insight into the physiological significance of long primary dendrites in mitral cells, and provides evidence against the use of reduced single compartmental models to investigate network properties of cortical pyramidal neurons.

Keywords: olfactory processing, synchronization, modeling, gap junction, mitral cells

Introduction

Gap junctions (GJs) between neurons are ubiquitous (Connors and Long, 2004) and their many roles have been shown in both experiments and models (reviewed in Velazques and Carlen 2000). The overall effects caused by the presence of GJs in a neuronal network can be complex. Several factors such as coupling strength (Sherman and Rinzel, 1994), cell properties (Pfeuty et al., 2003), and location (Traub et al., 2002) combine to modulate cell firing properties. In fact, GJs have been shown to be involved in spike frequency modulation (Kepler et al., 1990; Lewis and Rinzel, 2000; Moortgat

et al., 2000), fast oscillations (Draguhn et al., 1998; Friedman and Strowbridge, 2003), and in promoting the entire range of synchronization properties, from perfect synchronization to phase locking to antisynchrony (Sherman and Rinzel, 1994; Chow and Kopell, 2000).

These studies indicate the increasing interest in understanding how GJs affect the dynamics of neuronal networks. This is particularly important because their precise role is difficult to investigate experimentally, since the exact location, especially within extensive dendritic trees and with respect to the recording site, is usually unknown. In the olfactory bulb, however, excitatory connections (Urban and Sakmann, 2002) and, in particular, electrical coupling between mitral cells

*To whom all correspondence should be addressed.

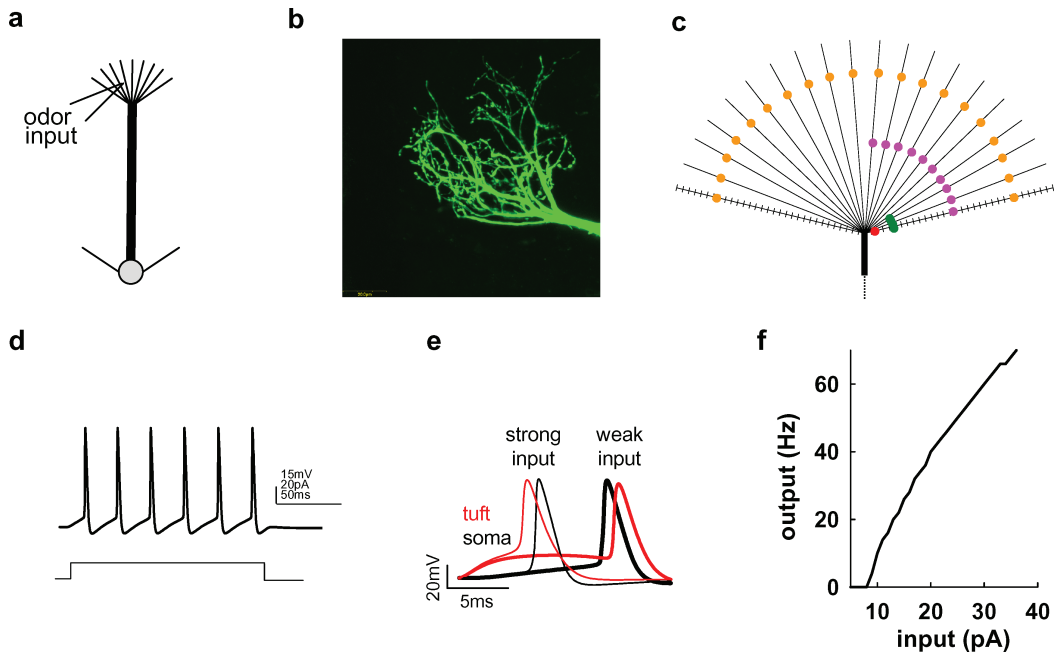
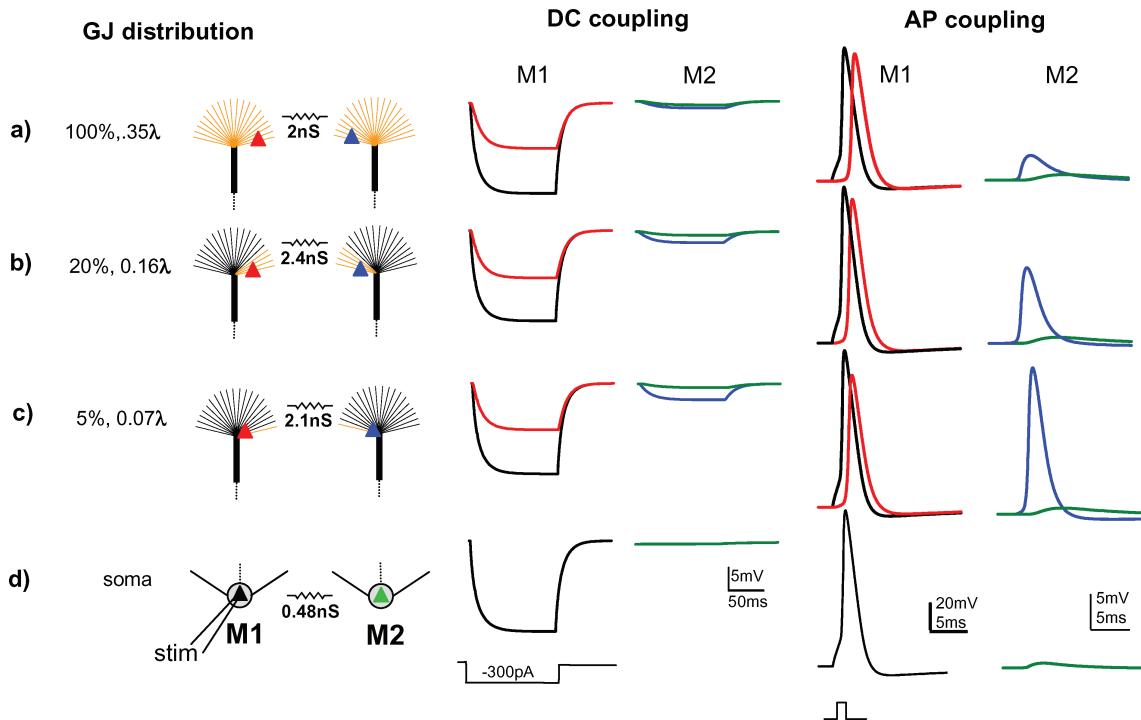


Figure 1. Basic properties of the model. (a) Schematic representation of the mitral cells used in the simulations; (b) Fluorescence image of a typical tuft of a mitral cell (courtesy of Zhishang Zhou, Yale University); (c) Schematic representation of the tuft geometry; each segment is 0.04λ long, and markers of different colors represent a few cases in which GJs were distributed on different portions (%) of the tuft (red: 5%, 0.08λ ; green: 20%, 0.2λ ; violet: 50%, 0.6λ ; orange: 100%, 1.0λ); (d) Somatic membrane potential during a step current injection in the tuft (20 pA, 150 ms); (e) membrane potential in the soma (black) and tuft (red, 0.3λ from primary dendrite) during a single activation of a weak (thick lines, 0.3 nA peak) or a strong (thin lines, 0.4 nA) tuft stimulation with a double-exponential current injection (2, and 5 ms for raise and decay time constants, respectively); (f) firing rate as a function of input current.



(Schoppa and Westbrook, 2002) has been experimentally observed only between cells projecting to the same glomerulus, suggesting that they are located in the tuft, making it a near ideal model system to study the effects of GJs. At the same time, it raises the question of how these distally-located GJs can control the synchronization of action potential output in the mitral cell axons.

Thus far there are limited insights into the roles of GJs in mitral cells compared with other neurons. The main suggestion thus far is that GJs provide for spread of the depolarization caused by activation of slow AMPA-like autoreceptors in the presynaptic cells (Schoppa and Westbrook, 2002). Building on this initial insight, we have asked what further functions might be mediated. An important recent finding is that the entire mitral cell dendritic tree (including the tuft) has been shown to have active properties (Bischofberger and Jonas, 1997; Debarbieux et al., 2003), with somatic action potentials propagating into the tuft at full amplitude (Debarbieux et al., 2003). A fundamental question therefore is how the function of gap junctions relates to these active properties?

To answer this question, we employ a realistic computational model of the mitral cell constrained by the experimental data. We first test the hypothesis that the GJs play a critical role in coupling action potential depolarization between the active dendritic tufts of mitral cells. We then test a second hypothesis that this coupling of action potentials in the distal tufts has a major role in promoting synchronization of mitral cell axonal output. We show that because the GJs are localized in the branches of the distal tuft they are electrotonically distant from the soma, allowing local processing of odor input before it reaches the soma. The fine branches have a high input resistance, which results in a local depolarization higher than that observed at the soma. The active properties provide a fast and efficient forward propagation of the synchronized spikes to the mitral cell somas and output through the axons. The model thus gives a physiologically plausible explanation for the development of long primary dendrites in mitral cells. It also provides evidence against the use

of reduced single compartmental models to investigate network properties of cortical pyramidal neurons.

Methods

All the simulations were carried out with the NEURON simulation program (Hines and Carnevale, 1997, ver. 5.5) using its variable time step feature and the *ParallelContext* class on a 24-processor cluster under PVM. In a few cases, simulations were carried out using a 512-processors IBM Linux cluster under MPI. The model and simulation files are available for public download under the ModelDB section of the Senselab database (<http://senselab.yale.med.edu>).

Circuit and Cell Properties

The canonical model used in all simulations was composed of 2 identical mitral cells (M1, M2). Each mitral cell (schematically represented in Fig. 1a) was implemented with an axon, soma, two secondary dendrites, and a primary dendrite connected to a tuft. For the tuft (Fig. 1b), except for the obvious presence of many small dendritic processes that in general may be electrotonically distant from the branch point with the primary dendrite, there is no detailed information on its morphology. Thus, any specific implementation would be arbitrary. However, experiments showing simultaneous dendritic and somatic mitral cell recordings, following a short electrical stimulation of the olfactory nerve (Chen et al., 2002), showed a smooth dendritic depolarization of the distal primary dendrite leading to a somatic or dendritic action potential. This suggests that there is no impedance mismatch between the tuft and the primary dendrite and that, in principle, the tuft could be modeled as a simple prolongation of the primary dendrite with an equivalent cable. However, we were interested in modeling the effects of placing gap junctions in different portions of the tuft. In this case, the effects of small dendrites, which present a higher input resistance, could be relevant.

For these reasons, we implemented the tuft using 20 identical thin compartments connected to the primary

Figure 2. Model's implementation of the experimental protocol used to study GJs in mitral cells (Schoppa and Westbrook, 2002) under different conditions of GJs location along the tuft and percent of dendrites connected. (*left*) Schematic representation of the different connections between the two mitral cells (M1, M2) used for the simulations on the right; in each case, the total GJ conductance, GJ location along the tuft, and percent of dendrites connected is indicated; markers indicate different recording locations (black: M1—soma, red: M1—tuft, blue: M2—tuft, green: M2—soma). (*middle*) membrane potential of different compartments during an hyperpolarizing somatic current injection in M1 (-0.3 nA, 150 ms). Lines color corresponds to the markers shown on the left. (*right*) membrane potential in the tuft (blue) and soma (green) of M2 during a short suprathreshold somatic current injection in M1 (1.5 nA, 1.5 ms). Coupling ratio is 0.04 in all cases.

dendrite (Fig. 1c), with diameters adjusted to follow the 3/2 branching rule ($0.4 \mu\text{m}$, in our case), and length equivalent to $\sim 1.3\lambda_{50}$, where λ_{50} was the space constant calculated at 50 Hz (Hines and Carnevale, 2001, $300 \mu\text{m}$ in our case). Uniform passive properties were used, with $R_a = 150 \Omega \cdot \text{cm}$, $\tau_m = 20 \text{ ms}$, and R_m and C_m adjusted to obtain an input resistance of about $100 \text{ M}\Omega$ (Mori et al., 1981). Resting potential was set at -65 mV and temperature at 35°C . Cells were modeled as regular firing cells (Fig. 1d), with Na , K_A , and K_{DR} conductances uniformly distributed over the entire dendritic tree (Bischofberger and Jonas, 1997; Debarbieux et al., 2003). Kinetics for the Na conductance were from CA1 hippocampal neurons (Migliore et al., 1999), whereas those for K_A and K_{DR} were from mitral cell data (Wang et al., 1996). Somatic action potentials backpropagated at full amplitude up to the tuft (Debarbieux et al., 2003), and AP could also initiate in the tuft or in the primary dendrite for moderate to strong odor inputs (Chen et al., 1997), as shown in the simulations in Fig. 1e. Odor inputs were modeled using long (1 sec) pulses of current injections in all tuft compartments at $\sim 0.35\lambda_{5w}$ from the branch point with the primary dendrite. This resulted in the mitral cells firing within the range of experimentally observed firing rates (Fig. 1f).

It should be noted that a number of additional mechanisms were not included in our model. Virtually all of them, such as subthreshold oscillations, additional K^+ conductances, persistent Na^+ current, Ca^{2+} -dependent currents, but also activity-dependent changes in channels density or kinetic, non-uniform distribution of the various Ca^{2+} currents, intracellular Ca^{2+} dynamics, etc., may modulate the synchronization process. This is precisely why we did not include them in the model, at this stage. Rather, we were interested in focusing on the specific role of action potential coupling mediated by GJs in the tuft, a process that is quite difficult to study experimentally. For these reasons, only those mechanisms needed for action potential generation have been included. It would be interesting to include additional cell properties in a future study, to investigate how and to what extent they affect the basic findings shown in this paper.

Gap Junction (GJ)

We modeled the current generated by a gap junction (GJ) as $I_{\text{GJ}} = g_{\text{gap}} \cdot (v_{\text{post}} - v_{\text{pre}})$, where g_{gap} , v_{post} , and v_{pre} , are the GJ conductance, the post- and the pre-synaptic membrane potential, respectively. There

is no indication from experiments on the dendritic location and total conductance. However, two experimental findings can be used to constrain the parameter space: (1) an action potential elicited in a cell should result in a somatic depolarization $\sim 1 \text{ mV}$ in a connected cell (Schoppa and Westbrook, 2002; Urban and Sakmann, 2002), and (2) the somatic voltage deflections observed with hyperpolarizing current injections in a test versus a stimulated cell should result in a coupling ratio (CR) in the range $0.01 < \text{CR} < 0.08$ (Schoppa and Westbrook, 2002). In most cases, the location within the tuft, the percentage of the dendrites connected, and the total GJ conductance were systematically explored and, in all cases, the main findings are presented and discussed for the cases that were consistent with the experimental findings.

In the experiments (Schoppa and Westbrook, 2002), a small ($< 0.15 \text{ mV}$, $< 1 \text{ ms}$) rapid deflection of the somatic membrane potential of the test cell was also observed at a short latency, with respect to an AP elicited in the stimulated cell. This deflection was interpreted as the ‘‘spikelet’’ resulting from the GJ coupling, in analogy with what observed in hippocampal cells (MacVicar and Dudek, 1982; Vigmond et al., 1997). However, the short latency and time course observed in the mitral cells case are inconsistent with the basic theory of signal spread in a dendritic tree (Rall, 1969), which predicts that a distal signal (such as that generated by a GJ in the tuft) will be delayed, reduced, and slowed as it spreads passively toward the soma. In fact, in hippocampal cells, spikelets are much larger ($> 1 \text{ mV}$) and most likely caused by axo-axonal GJs (Traub et al., 2003). Furthermore a detailed model of the electrical coupling between pyramidal cells (Vigmond et al., 1997) suggested that a rapid deflection such as that observed in mitral cells could be caused by the electric field of a single source cell. For these reasons, our model did not take into account this effect.

Results

The number and distribution of GJs connecting the tuft dendrites of two mitral cells is unknown, as is the electrotonic distance between the recording site and the GJs location (soma and tuft, respectively). There could therefore be a number of different combinations of GJ strengths and distributions that could be consistent with the experimental findings. In Fig. 2 we explore several relevant possibilities. The GJs were distributed in different ways within the tuft, as schematically

represented in Fig. 2 left, and in each case the voltage deflections at different locations (Fig. 2, markers) are shown during a somatic stimulation of M1 with a hyperpolarizing current injection (Fig. 2, DC coupling, -0.3 nA 150 ms) or with a brief suprathreshold current pulse (Fig. 2, AP coupling, 1.5 nA, 1.5 ms). For comparison, we also included the unrealistic assumption (but widely used in network simulations of gap junctional coupling between neurons) of a somatically located input and GJ.

In all simulations, the total GJ conductance was adjusted in such a way to be consistent with the experimental findings of a $CR = 0.04$ and a peak somatic depolarization of ~ 1 mV (see Methods). The first result was that to meet these two conditions, approximately the same total GJ conductance (~ 2 nS) could be used for GJs wherever located in the tuft. Assuming a unitary channel conductance of 10–15 pS for GJs formed by Connexin 36 (Teubner et al., 2000) this value corresponds to the opening of 100–150 individual channels. By comparison, a much lower value (0.475 nS, corresponding to 32–48 open channels) was obviously required for the unrealistic case of coupling of the somas through a somatic GJ. The second result was that even if an AP in M1 resulted in the same small M2 somatic depolarization (Fig. 2, AP coupling, green lines) the local tuft depolarization varied widely depending on the specific GJ connectivity (Fig. 2, AP coupling, blue lines). There was a smaller depolarization when GJs were distributed over the entire tuft (~ 5 mV, Fig. 2a), and a much higher depolarization for localized GJs (~ 20 mV, Fig. 2c). These results indicated that the distal tuft branches are sensitive sites for regulating the local coupling between the mitral cells, without having differential effects on distant somatic coupling potentials.

To examine more closely the effects of the tuft regulation as seen at the somas, in Fig. 3 we compared the different somatic depolarizations under the different conditions of GJ coupling in the tufts from Fig. 2 (green traces at far right). The brief transient current, generated in M2 through the GJ connections by an AP in M1, caused a somatic depolarization that, with respect to the AP in M1 (Fig. 3A, dashed line), peaked at different latencies as the GJs were moved from the soma to more distal locations in the tuft. As expected from cable properties affecting subthreshold signal propagation in a dendritic tree (Rall, 1969; Johnston and Wu, 1995), and consistent with what has already been pointed out in a detailed modeling study of electrical coupling between pyramidal cells (Vigmond et al., 1997), the GJs

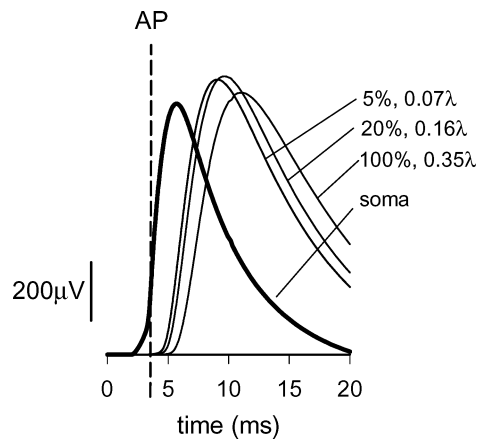


Figure 3. Somatic depolarization induced in M1 by eliciting an AP in M2. (top) Modeling results: expanded view of the somatic depolarization from Fig. 2. The GJ location along the tuft, and percent of dendrites connected is indicated. The dashed line indicates the time of AP peak in M1; Coupling ratio is 0.04 in all cases.

in the tuft resulted in a somatic depolarization with a latency and decay time determined by the cell properties and GJ locations. These depolarizations were very similar to the average AMPA-like synaptic EPSP observed experimentally (Schoppa and Westbrook, 2002). Although a direct comparison between model and experimental traces was not possible (it would require much more detailed information on the experimental conditions), these results suggest that these depolarizations could be due to the APs propagating through the GJs in the tuft, and support the view that they play an important role in intraglomerular coupling.

In the experiments (Schoppa and Westbrook, 2002), the somatic depolarization attributed to GJs in the tuft was very small (a 0.1 mV spikelet). We then studied if this effect could result at the same time in a coupling ratio within the experimentally observed range ($0.01 < CR < 0.08$). A series of simulations were thus carried out by finding, for each combination of extent of dendrites connected by GJs and distance within the tuft to the site of branching from the primary dendrite, the GJ conductance needed to obtain a 0.1 mV depolarization at the soma. This conductance was then used in each case to calculate the CR using the hyperpolarization protocol as in Fig. 2 (DC coupling). The results are summarized in the contour plot in Fig. 4, and show that the CR was negligible (< 0.001) in all cases, suggesting that a 0.1 mV somatic depolarization caused by a GJs coupling in the tuft cannot result in a CR within the experimentally observed range.

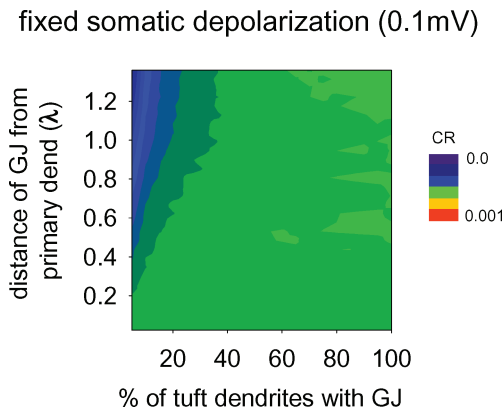


Figure 4. Coupling ratio at the soma when AP coupling caused a GJs mediated somatic depolarization of 0.1 mV as a function of the percentage of tuft dendrites connected by a GJ (abscissa) at different electrotonic distances from the branch point with the primary dendrite (ordinate).

The next question addressed was what possible GJ distributions were consistent with the experiments. To answer this we carried out an extensive series of simulations in which we varied the location of GJs within the tuft and the extent of dendrites interconnected, under the constraint of the coupling ratio as seen at the soma of $CR = 0.04$. The results are summarized in the contour plots in Fig. 5. The red areas represent values of the parameters for which an AP was generated in M2. The results show that there was a wide range of GJ distributions that were consistent with the experimental findings of a somatic depolarization $0.6 < V_{soma} < 1$ mV (Fig. 5, left, light blue and green areas). The same CR could be obtained with GJs close to the primary

dendrite but connecting only a few dendrites (lower left corner of contour plot) or with GJs distributed throughout the entire tuft. Under these conditions, the peak dendritic depolarization was always >2.5 mV, and spanned a wide range of subthreshold values (Fig. 5, middle, blue and green areas). The total GJ conductance needed in each case to satisfy $CR = 0.04$ (Fig. 5, right) was within the theoretical limit for a GJ, as estimated by ultrastructural studies (~ 5 nS, Fukuda and Kosaka, 2003, corresponding to 350–500 channels). In summary, the distribution of GJs within the tuft cannot be inferred from somatic recordings (this is discussed further in the Discussion).

Synchronization

What is the significance of AP synchronization at the soma and axonal output between neurons through distally-located dendritic GJs? This is obviously a critical question for odor processing in the olfactory bulb, and may be a more general phenomenon.

The synchronization test system is shown in Fig. 6. In the simulation illustrated in Fig. 6, M1 (black line) and M2 (red line) receive the same current injection (20 pA) but starting with a 10 ms relative delay. Under control conditions of no coupling (Fig. 6A), the two cells fire independently and do not, of course, show any synchronization. The addition of a GJ (100%, $1.3\lambda_{5w}$, $CR = 0.03$) resulted in cell synchronization (Fig. 6B). The GJ current was rather large at the beginning of the stimulation, when the two cells were not synchronized. The current direction was determined by the relative

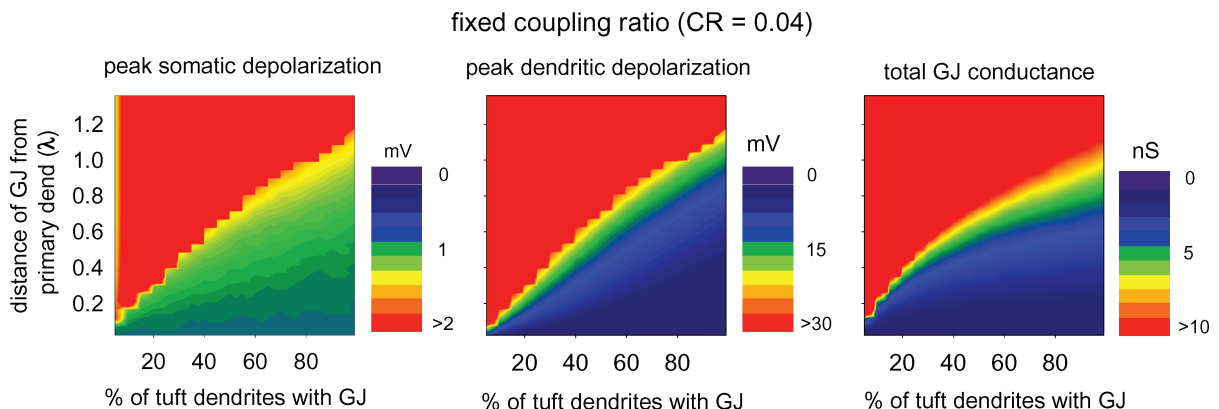


Figure 5. Depolarization in M2 induced by an AP in M1. The contour plots show the peak depolarization at the soma (left), the local peak depolarization in the tuft (middle), and the total GJ conductance (right) as a function of the percentage of tuft dendrites connected by GJ at different electrotonic distances from the branch point with the primary dendrite. Coupling ratio is 0.04 in all cases.

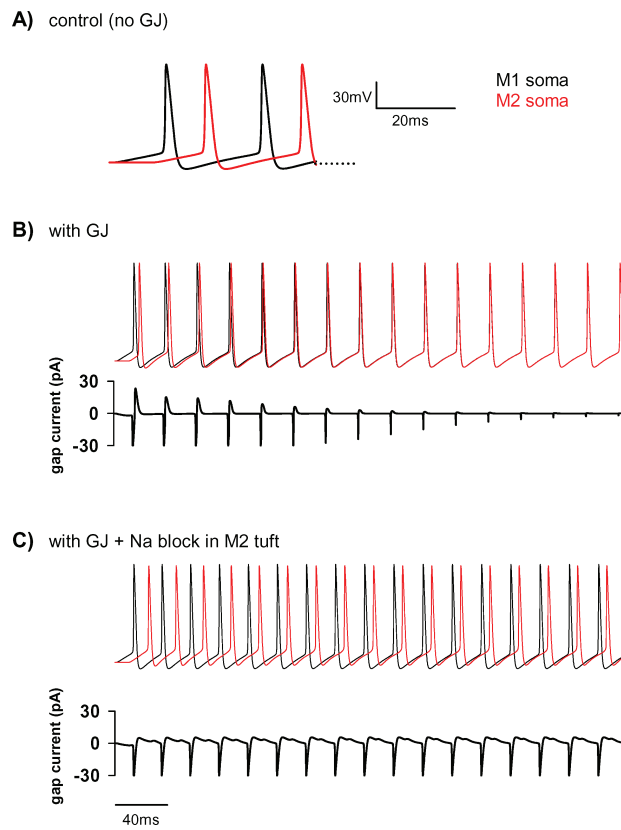


Figure 6.

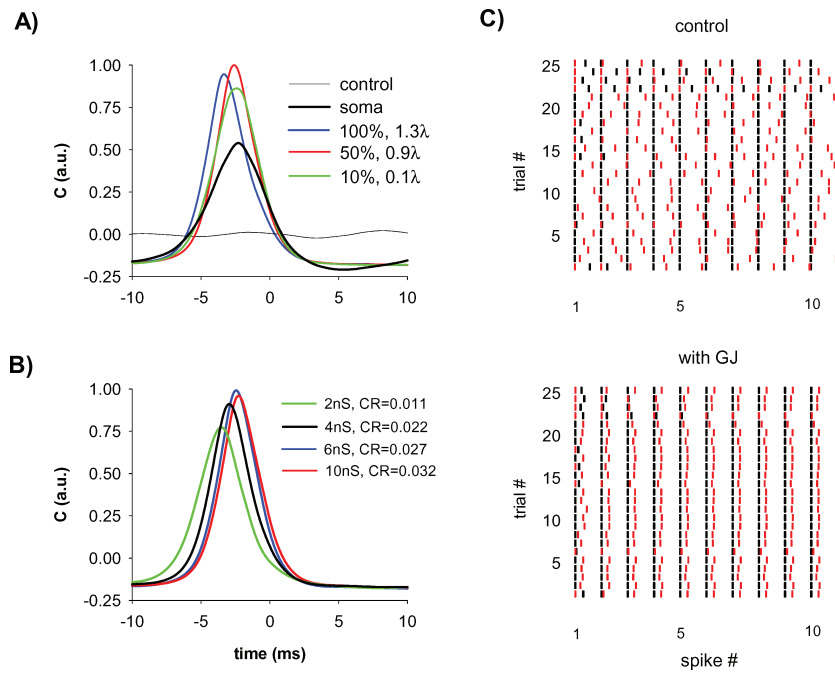


Figure 7.

difference in the local (tuft) membrane potential between the two cells, and altered the spike times of each cell until synchronization took place. As synchronization occurred, the GJ current decreased to near zero, because there was no net current between the two simultaneously firing cells. The active properties of the tuft might have an important role in the synchronization properties and the model suggests the experimentally testable prediction that blocking Na channels (required for AP generation) in one of the cell should interfere with the synchronization process. In the simulation of Fig. 6C, Na⁺ channels were blocked only in the tuft of M2. Under these conditions, somatic action potentials were still elicited in M2 (Fig. 6C, red line) but a substantial portion of the GJ current was lost (since APs could not propagate or be generated in the M2 tuft) and the two cells could not synchronize. These results clearly showed that GJs and active properties constrained by the experimental parameters are able to mediate AP synchronization for the case of the same inputs with delays.

In the more general case likely to occur *in vivo* M1 and M2 may be assumed to receive a different input to their distal dendrites. The way in which two cells can become synchronized under these conditions is very difficult to study experimentally. In the model, this was studied by calculating the cross-correlation of M1 and M2 somatic membrane potentials (Fig. 7A and B), under different GJ distributions while still meeting the constraint of a peak somatic depolarization of ~ 1 mV. Each curve was the average of 25 simulations in which both the input strength and starting times were drawn from a uniform random distribution within the intervals 20 ± 2 pA and 0–12 ms, respectively, and in all cases M1 received the higher input and was chosen as reference. We first studied some typical cases in which GJs produced a peak dendritic depolarization of ~ 20 mV

(Fig. 7A). No correlation was found under control conditions, and GJs in the tuft always resulted in better synchronization with respect to a GJ in the soma. The different GJ distributions in the tuft resulted in similar peak cross-correlation values and phase shift between the reference and the test cell, with the cell receiving the higher input firing a few ms before the other cell. Because the correlation properties could also depend on the coupling strength we also tested different GJ conductances (Fig. 7B, GJs in 50% of the tuft, at $0.9\lambda_{5w}$ from branch point with the primary dendrite). The cross-correlation curves differed little. Only for a very weak coupling (0.2 nS and CR = 0.011, close to the lowest experimentally measured of CR = 0.012) was a significant reduction in the cross-correlation peak ($\approx 25\%$) and a larger spike time difference (≈ 4 ms) observed. These results thus show that the GJs in the tuft play a major role in MC synchronization over a broad range of distributions in the tuft, different strengths of inputs, and different input latencies.

To visualize the GJ effects, in Fig. 7C we present the raster plots of the first 10 spike times for 25 trials (simulations) under control conditions (Fig. 7C, top) and with GJ (Fig. 7C, bottom, 50%, $0.9\lambda_{5w}$). In all cases black markers show the spike times of the cell receiving the higher input (M1), whereas the spike times of the other cell (M2) are shown in red. In order to illustrate better the differences between the two conditions, the n -th spike times were independently aligned to the n -th spike time of the cell firing first across all trials, and successive spikes during each trial (Fig. 7C, abscissa) were arbitrarily spaced by 10 ms. Thus, in these plots, only the relative time difference between the n -th spikes of the two cells was significant. The effect of the GJ was striking (Fig. 7C, bottom). After just a couple of spikes the cell receiving the higher input (black) always fired a few ms before the other one (red),

Figure 8. Synchronization process for M1 and M2 receiving the same input current (0.2 nA) starting with a 10 ms delay. (A) Somatic membrane potential of M1 (black) and M2 (red) under control conditions; (B) Somatic membrane potential of M1 (black) and M2 (red) with GJ (total cond. 7.2 nS) connecting 100% of M1 and M2 tuft dendrites at $1.3\lambda_{5w}$; (C) Same in (B) but with no sodium channels in the tuft dendrites of M2.

Figure 9. Cross correlation of 0.5 sec recordings of M1 and M2 somatic membrane potential from 25 simulations. Input currents and relative latency in each simulation were drawn from a uniform random distribution within the intervals 18–22 pA and 0–12 ms, respectively. (A) Normalized average cross correlation (c , in arbitrary units, a.u.): (thin black line) control (no GJ); (thick black line) GJ and input at the soma; (blue) M1 and M2 tufts fully connected with GJ at $1.3\lambda_{5w}$ from branch point; (red) 50% of M1 and M2 tufts connected with GJ at $0.9\lambda_{5w}$; (green) 10% of M1 and M2 tufts connected with GJ at $0.1\lambda_{5w}$ or the cases of GJ in the tuft, the peak M2 tuft and somatic depolarization was ~ 20 and ~ 1 mV, respectively. (B) As in (A) but, in all cases, 50% of M1 and M2 tufts were connected with GJs at $0.9\lambda_{5w}$. (C) raster plots of the first 10 spike times over the 25 trials under control conditions (top) and with GJ (bottom, 50%, $0.9\lambda_{5w}$). Black markers: spike times of the cell receiving the higher input; Red markers: spike times of the cell receiving the weaker input. The same input was used for the same trial under different conditions. See text for details on how the plots were arranged.

even when the cell receiving the weaker input was firing first at the beginning of the simulation (see spike #1 for trials 1, 6, 14, 16, 18, and 22–25 in control).

Discussion

In a realistic model of electrically connected mitral cells we have shown that the somatically-measured experimental properties of GJs may correspond to a variety of different local coupling strengths and dendritic distributions of GJs in the tuft. The model suggested that the somatic depolarization caused in the test cell by GJ coupling, as constrained by the experimental findings, is practically indistinguishable from an AMPA-like EPSP, in agreement with another study (Vigmond et al., 1997). We thus propose that the propagation of the GJ-induced local depolarization is the major component of the experimentally-observed somatic depolarization. Of course, this does not exclude the activation of slow AMPA autoreceptors, but the model predicts that they would not be necessary for synchronization. In the experiments, the involvement of glutamatergic transmission was inferred from the effects of the AMPA/kainate receptor antagonist NBQX (Schoppa and Westbrook, 2002), which nearly abolished the somatic depolarization in the test cell. Because in our model the somatic depolarization is caused by the GJ alone, this implies the interesting possibility that the intraglomerular GJ coupling might be directly or indirectly affected by pharmacological manipulations of the neurotransmitter/neuromodulator-related processes. A detailed discussion of the biochemical processes that could be involved in this modulation is outside the scope of the present paper. It should be stressed, however, that there is experimental evidence for glutamate-dependent modulation of the GJ conductance (reviewed in Hatton, 1998). In mitral cells belonging to the same glomerulus, this effect could be experimentally tested by comparing the DC coupling (as in Fig. 2) before and after application of glutamate receptor antagonists.

Synchronization

Previous studies of cell synchronization in the olfactory bulb have provided information on mechanisms such as lateral inhibition (Linster and Hasselmo, 1997; Urban, 2002; Davison et al., 2003), oscillating subthreshold

inputs (e.g. Margrie and Schaefer, 2003), and more general computational issues (Haberly, 2001; Laurent et al., 2001; Brody and Hopfield, 2003). In all cases, the focus has been on the inhibitory mechanisms mediated by granule cell activation. In this work we focused on the role of GJs in a reduced glomerular unit, consisting of two interconnected mitral cells, as key to synchronization mechanisms. The model predicts that, in spite of the observed small somatic coupling ratio, GJs are sufficient for synchronization of mitral cells. The effect is robust for the entire range of somatic coupling ratio experimentally measured, is caused by the much larger local coupling in the tuft (Fig. 5), and is supported by the active properties in the tuft (Fig. 6). The GJs' strategic position (where odor input arrives) and its working range (any difference in the membrane potential between the two connected cells will immediately generate a gap coupling) make them the first mechanism to promote mitral cells synchronization during odor responses. In fact, they could have an instrumental role to spread and "equalize" the tuft depolarization among the mitral cells belonging to the same glomerulus even before it reaches the soma or generate an action potential. This may critically control the initial processing of odor input before the network of granule cells, that connect the mitral cell secondary dendrites, becomes involved, and could explain the experimental observation that synchronization is not sensitive to the block of inhibition of mitral cells connected by GJs (Schoppa and Westbrook, 2002). According to our findings, the GJs may act to merge the inputs received from differently-activated ORNs to synchronize the activated mitral cells within a glomerular unit (i.e., all cells connected to a given glomerulus). This can be regarded as effectively implementing a many-are-equal (MAE) kind of computation (Hopfield and Brody, 2000, 2001; Brody and Hopfield, 2003) at the initial stage of odor processing. Further intraglomerular processing within the glomerular unit, due to the local inhibitory mechanisms caused by the activation of different interneuron populations (e.g. periglomerular and juxtglomerular cells), could be expected to modulate the range of inputs for which synchronization could be achieved. Their role and interaction with GJs will be the subject of a future study.

For our study we have used the values for GJ coupling obtained in physiological experiments. For wider application of these results it should be noted that the experiments were carried out in slices obtained from young animals. Extrapolation to mature animals of

many months therefore must be done with caution. Although serial electron microscopical reconstructions have shown intraglomerular GJs between mitral cells in 2-month old mice (Kosaka and Kosaka, 2004), there is a general tendency for gap junctional coupling to be highest during early development. It may be thus hypothesized that GJ coupling plays a leading role in synchronizing mitral cells during early development, with other mechanisms involving synaptic inhibition playing an increasing role with aging. Interactions between electrical and chemical synaptic coupling therefore will be of increasing importance.

In this study we have focused on synchronization *per se*. Further studies will be required to relate these mechanisms to the generation of different types of synchronous oscillatory activity that may be found in the olfactory bulb under different conditions of sensory stimulation and centrifugal control.

Comparisons with Other Systems

Much of the current interest in synchronization through gap junctions in the mammalian brain is focused on inhibitory interneurons (Galarreta and Hestrin, 2001). By contrast, there are only a few cases of GJs between principal neurons (such as mitral cells). Historically, the best known is the inferior olive, in which gap junctions between the principal cells are located between distal dendrites that shunt excitatory synaptic inputs (reviewed in Llinas et al. 2002), and axonal GJs between hippocampal CA1 pyramidal neurons has been suggested as a novel source of fast network oscillations (reviewed in Traub et al., 2002). This type of interaction deserves further study in the mitral cell tuft.

Considerations of Large Scale Networks

Our results in the mitral cell have further general relevance to neural network simulations. To reduce simulation time or to allow analytical investigation of the equations involved, individual neurons are customarily implemented in large networks using reduced single compartment (“isoelectrotonic”) units representing the entire neuron with its dendritic tree. Although this could be appropriate in studying network properties caused by events occurring (electrotonically) close to the soma, neurons with extensive dendritic trees cannot be easily reduced in this way, unless the overall effect has been previously assessed in a realistic model and then (if possible) adequately reproduced in a reduced

model. This is particularly important for the case of GJs between mitral cells, for which there is clear experimental evidence of their localization in the tuft, far from the soma. This actual distance is 300–500 microns in the rat, with the electronic length of the order of 1 (see Shepherd et al., 2004). An investigation of the conditions under which a realistic model of a mitral cell could be reduced to a minimal implementation, preserving the same basic properties, is outside the scope of this work. However, our findings suggested one of the possible problems in using a somatic GJ (as in single compartment models) rather than in the tuft. By using a somatic GJ, and taking into account the experimental constraints, the effective coupling between the two cells will be greatly underestimated (Fig. 2). The end result will be a much weaker effect of GJ on synchronization (Fig. 7), which cannot be compensated by simply increasing the GJ conductance, since this will produce a higher somatic depolarization. In addition to being inconsistent with experiments, this could also be expected to interfere with the other mechanism that is widely assumed to have a major role in mitral cell synchronization as well as other properties, i.e. inhibition through granule cells. We thus have a persuasive functional rationale for the development of an elongated primary dendrite ending with a tuft: to separate intraglomerular local processing of odor input coming from a homogeneous population of ORNs within the same glomerular unit, from interglomerular processing underlying odor recognition and discrimination occurring at a later stage mediated by granule cells and involving many glomerular units (cf. Davison et al., 2003).

Acknowledgments

We are grateful for support by National Institutes of Health Grant DC-00086, the Human Brain Project (National Institute of Deafness and Other Communication Disorders, National Institute of Mental Health, National Institute of Neurological Disorders and Stroke, and National Institute on Aging), the Office of Naval Research (Multiuniversity Research Initiative NINDS Grant NS11613), and CINECA (for access to the 512-processors IBM linux cluster). We thank W. Chen, T. Morse, and P.-M. Lledo for valuable discussions.

References

- Bischofberger J, Jonas P (1997) Action potential propagation into the presynaptic dendrites of rat mitral cells. *J. Physiol.* 504: 359–365.

- Brody CD, Hopfield JJ (2003) Simple networks for spike-timing-based computation, with application to olfactory processing. *Neuron* 37: 843–852.
- Chen WR, Shen GY, Shepherd GM, Hines ML, Midtgaard J (2002) Multiple modes of action potential initiation and propagation in mitral cell primary dendrite. *J. Neurophysiol.* 88: 2755–2764.
- Chow CC, Kopell N (2000) Dynamics of spiking neurons with electrical coupling. *Neural Comput.* 12: 1643–1678.
- Connors BW, Long MA (2004) Electrical synapses in the mammalian brain. *Annu. Rev. Neurosci.* 27: 393–418.
- Davison AP, Feng J, Brown D (2003) Dendrodendritic inhibition and simulated odor responses in a detailed olfactory bulb network model. *J. Neurophysiol.* 90: 1921–1935.
- Debarbieux F, Audinat E, Charpak S (2003) Action potential propagation in dendrites of rat mitral cells in vivo. *J. Neurosci.* 23: 5553–5560.
- Draguhn A, Traub RD, Schmitz D, Jefferys JG (1998) Electrical coupling underlies high-frequency oscillations in the hippocampus in vitro. *Nature* 394: 189–192.
- Friedman D, Strowbridge BW (2003) Both electrical and chemical synapses mediate fast network oscillations in the olfactory bulb. *J. Neurophysiol.* 89: 2601–2610.
- Galarreta M, Hestrin S (2001) Electrical synapses between GABA-releasing interneurons. *Nat. Rev. Neurosci.* 2: 425–433.
- Haberly LB (2001) Parallel-distributed processing in olfactory cortex: New insights from morphological and physiological analysis of neuronal circuitry. *Chem. Senses* 26: 551–576.
- Hatton GI (1998) Synaptic modulation of neuronal coupling. *Cell Biol. Intern.* 22: 765–780.
- Hines M, Carnevale T (1997) The NEURON simulation environment. *Neural Comp.* 9: 178–209.
- Hines ML, Carnevale NT (2001) NEURON: A tool for neuroscientists. *Neuroscientist* 7: 123–135.
- Hopfield JJ, Brody CD (2000) What is a moment? “Cortical” sensory integration over a brief interval. *Proc. Natl. Acad. Sci. USA* 97: 13919–13924.
- Hopfield JJ, Brody CD (2001) What is a moment? Transient synchrony as a collective mechanism for spatiotemporal integration. *Proc. Natl. Acad. Sci. USA* 98: 1282–1287.
- Johnston D, Wu SM (1995) Functional properties of dendrites. In: *Foundation of Neurophysiology*. MIT Press, Cambridge, Ch. 4.
- Kepler TB, Marder E, Abbott LF (1990) The effect of electrical coupling on the frequency of model neuronal oscillators. *Science* 248: 83–85.
- Kosaka T, Kosaka K (2004) Neuronal gap junctions between intraglomerular mitral/tufted cell dendrites in the mouse main olfactory bulb. *Neurosci. Res.* 49: 373–378.
- Laurent G, Stopfer M, Friedrich RW, Rabinovich MI, Volkovskii A, Abarbanel HD (2001) Odor encoding as an active, dynamical process: Experiments, computation, and theory. *Ann. Rev. Neurosci.* 24: 263–297.
- Lewis TJ, Rinzel J (2000) Self-organized synchronous oscillations in a network of excitable cells coupled by gap junctions. *Network* 11: 299–320.
- Linster C, Hasselmo M (1997) Modulation of inhibition in a model of olfactory bulb reduces overlap in the neural representation of olfactory stimuli. *Behav. Brain Res.* 84: 117–127.
- Llinas R, Leznik E, Makarenko VI (2002) On the amazing olivocerebellar system. *Ann. N. Y. Acad. Sci.* 978: 258–272.
- MacVicar BA, Dudek FE (1982) Electrotonic coupling between granule cells of rat dentate gyrus: Physiological and anatomical evidence. *J. Neurophysiol.* 47: 579–592.
- Margrie TW, Schaefer AT (2003) Theta oscillation coupled spike latencies yield computational vigour in a mammalian sensory system. *J. Physiol.* 546: 363–374.
- Migliore M, Hoffman DA, Magee JC, Johnston D (1999) Role of an A-type K⁺ conductance in the back-propagation of action potentials in the dendrites of hippocampal pyramidal neurons. *J. Comput. Neurosci.* 7: 5–15.
- Moortgat KT, Bullock TH, Sejnowski TJ (2000) Gap junction effects on precision and frequency of a model pacemaker network. *J. Neurophysiol.* 83: 984–997.
- Mori K, Nowycky MC, Shepherd GM (1981) Electrophysiological analysis of mitral cells in the isolated turtle olfactory bulb. *J. Physiol.* 314: 281–294.
- Perez Velazquez JL, Carlen PL (2000) Gap junctions, synchrony and seizures. *Trends Neurosci.* 23: 68–74.
- Pfeuty B, Mato G, Golomb D, Hansel D (2003) Electrical synapses and synchrony: The role of intrinsic currents. *J. Neurosci.* 23: 6280–6294. Erratum In: *J. Neurosci.* 23: 7237.
- Rall W (1969) Time constants and electrotonic length of membrane cylinders and neurons. *Biophys. J.* 9: 1483–1508.
- Schoppa NE, Westbrook GL (2002) AMPA autoreceptors drive correlated spiking in olfactory bulb glomeruli. *Nat. Neurosci.* 5: 1194–1202.
- Shepherd GM, Chen WR, Greer CA (2004) Olfactory bulb. In *The Synaptic Organization of the Brain* (Fifth Edition) ed. Shepherd, GM. New York: Oxford University Press, pp. 165–216.
- Sherman A, Rinzel J (1992) Rhythmogenic effects of weak electrotonic coupling in neuronal models. *Proc. Natl. Acad. Sci. USA* 89: 2471–2474.
- Teubner B, et al (2000) Functional expression of the murine connexin 36 gene coding for a neuron-specific gap junctional protein. *J. Membr. Biol.* 176: 249–262.
- Traub RD, Draguhn A, Whittington MA, Baldeweg T, Bibbig A, Buhl EH, Schmitz D (2002) Axonal gap junctions between principal neurons: A novel source of network oscillations, and perhaps epileptogenesis. *Rev. Neurosci.* 13: 1–30.
- Traub RD, Pais I, Bibbig A, LeBeau FE, Buhl EH, Hormuzdi SG, Monyer H, Whittington MA (2003) Contrasting roles of axonal (pyramidal cell) and dendritic (interneuron) electrical coupling in the generation of neuronal network oscillations. *Proc. Natl. Acad. Sci. USA* 100: 1370–1374.
- Urban NN (2002) Lateral inhibition in the olfactory bulb and in olfaction. *Physiol. Behav.* 77: 607–612.
- Urban NN, Sakmann B (2002) Reciprocal intraglomerular excitation and intra- and interglomerular lateral inhibition between mouse olfactory bulb mitral cells. *J. Physiol.* 542: 355–367.
- Vigmond EJ, Perez Velazquez JL, Valiante TA, Bardakjian BL, Carlen PL (1997) Mechanisms of electrical coupling between pyramidal cells. *J. Neurophysiol.* 78: 3107–3116.
- Wang XY, McKenzie JS, Kemm RE (1996) Whole-cell K⁺ currents in identified olfactory bulb output neurones of rats. *J. Physiol.* 490: 63–77.